PERGAMON

International Journal of Multiphase Flow 24 (1998) 855–866

International Journal of Multiphase Flow

Brief Communication

Pressure wave speeds from the characteristics of two fluids, two-phase hyperbolic equation system

Sung-Jae Lee [a], Keun-Shik Chang [b,*], Kyungdoo Kim [a]

[a] Korea Atomic Energy Research Institute, Thermo-hydraulic Research Team, Yusung-ku, Taejon 305-353, Korea
[b] Korea Advanced Institute of Science and Technology, Aerospace Engineering Department, 373-1 Kusong-Dong, Yusung-Ku, Taejon 305-701, Korea

Received 7 June 1997; received in revised form 25 November 1997

1. Introduction

Considerable effort has been made in the past, without much success, to determine the pressure wave propagation speed for two fluids, two-phase flow. Delhaye et al. (1981) and Ishii (1975) have showed systematic derivation of the governing equations for two-phase flows. However, this governing equation system has complex characteristics, making the two-phase flow formulation mathematically ill-posed, see Ramshaw and Trapp (1978); Stewart (1979). Various modifications of the governing equations has therefore been followed to render the characteristic roots real.

The single-pressure models in the classical two fluids, two-phase formulation assume that the pressure is continuous across the interface boundary. Unfortunately, these models lead to the afore-mentioned complex eigenvalues for the practical problems under review. In contrast, the two-pressure models assume that the gas and the liquid pressures are not necessarily continuous across the interface. These models have, as a matter of fact, produced real eigenvalues, see Ransom and Hicks (1984); Holm and Kupershmidt (1986); Ramshaw and Trapp (1978). However, most of the two-pressure models are either deficient of the constraint binding the two phasic pressures, producing nonphysical behavior in the solution, or based on the pressure constraints true only for a particular type of two-phase flows.

To construct new two fluids and two-phase flow formulation, we consider one-dimensional mass and momentum conservation equations

$$\frac{\partial(\epsilon_k \rho_k)}{\partial t} + \frac{\partial(\epsilon_k \rho_k v_k)}{\partial x} = \phi_{c,k} \tag{1}$$

* To whom correspondence should be addressed.

PII: S0301-9322(97)00089-X

$$\frac{\partial(\epsilon_k\rho_k v_k)}{\partial t}+\frac{\partial(\epsilon_k\rho_k v_k^2)}{\partial x}+\epsilon_k\frac{\partial p_k}{\partial x}+(p_k-p_i)\frac{\partial\epsilon_k}{\partial x}=\phi_{m,k} \tag{2}$$

The subscript k is for either phase ($k = G,L$) and i is for the interface; ϵ, ρ, v are respectively the void fraction, the density, and the flow velocity. The source terms $\phi_{c,k}$ and $\phi_{m,k}$ on the right hand side of (1) and (2) do not affect the mathematical type of the partial differential equations. The above system of equations has more unknowns than the number of equations. The innovative feature of the present formulation is that we have introduced a small differential pressure force term, $(p_k-p_i)\partial\epsilon_k/\partial x$, as a force balance in the momentum equations. Although this term which will be derived from the surface physics shortly might be very small, it converts the equation system into hyperbolic type without introducing the virtual mass or artificial additive terms, unlike the earlier formulations.

2. Pressure constraint

For a sphere having an infinitely thin film of radius R and surface tension σ, the well-known Young and Laplace's formula becomes

$$p_G-p_L=\frac{2\sigma}{R} \tag{3}$$

For a very thin film of finite thickness δ, this equation should be modified to the form

$$p_G-p_L=\frac{2\delta}{R_G+\delta/2}\left(\frac{\sigma}{\delta}\right)=\frac{2\delta}{R_L-\delta/2}\left(\frac{\sigma}{\delta}\right) \tag{4}$$

where the radius R in (3) is replaced by $R_G+\delta/2$ or $R_L-\delta/2$ the distance from the center of the sphere to the half thickness of the thin film, or the average distance to the film; see Fig. 1. This

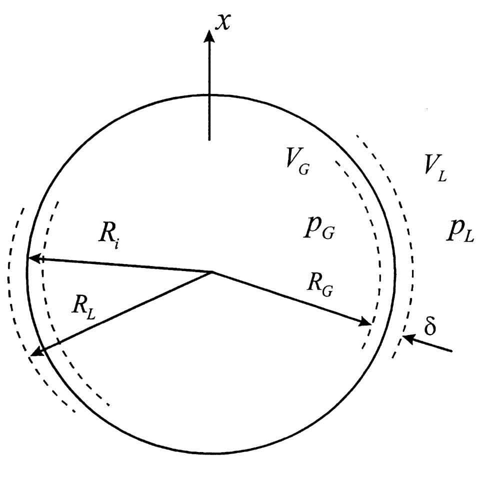

Fig. 1. Spherical interface model with finite thickness δ.

thin film of thickness δ can represent the hypothetical interfacial thickness estimated earlier in the statistical mechanics, see Clive (1980); Egelstaff and Widom (1970); Present (1974).

Let A_i and V_G denote respectively the surface area and the gas volume of the sphere with the interface film at the average distance $R_G + \delta/2$. When the radius of the sphere is changed by the increment ΔR_G, the surface area and the gas volume will be accordingly changed, satisfying

$$\frac{R_G}{2}\left(\frac{\Delta A_i}{\Delta V_G}\right) = 1 - \frac{\delta/2}{R_G + \delta/2} \tag{5}$$

For the liquid side, the above relation is subject to

$$\frac{R_L}{2}\left(\frac{\Delta A_i}{\Delta V_L}\right) = -1 - \frac{\delta/2}{R_L - \delta/2} \tag{6}$$

In the limit for $\Delta R_G \rightarrow 0$ with the total volume $V = V_L + V_G$, it holds that

$$\frac{\partial(A_i/V)}{\partial(V_L/V)} = \frac{\partial a_i}{\partial \epsilon_G} = -\frac{\partial a_i}{\partial \epsilon_L} \tag{7}$$

wherea_i is the interfacial area per unit volume. Equation (4) then becomes, upon using (5) and (7),

$$(p_G - p_L) = \left(\frac{4\sigma}{\delta}\right)\left(1 - \frac{R_G}{2}\frac{\partial a_i}{\partial \epsilon_G}\right) \tag{8}$$

The factor $4\sigma/\delta$ in the right hand side plays the role of a *Lagrangian multiplier* given in Papalambros and Douglass (1988) and Aubin and Ekeland (1984), which helps to identify a particular two-phase flow regime under consideration.

Relationship between the surface tension and the surface thickness has been sought for a long time. It is now known from the statistical mechanics and the physical chemistry that an approximation can be made as $C\sigma/\delta = L$. Here C is a constant and L is a bulk modulus. From this and the physics of surface tension at the interface where the density is discontinuous, the so-called bulk modulus, $4\sigma/\delta = L$, can be split into two parts as follows

$$\frac{4\sigma}{\delta} = L_G + L_L \tag{9}$$

By means of (5)–(7), (8) is changed to

$$(p_G - p_i) - (p_i - p_L) = L_G\left(1 - \frac{R_G}{2}\frac{\partial a_i}{\partial \epsilon_G}\right) - L_L\left(1 + \frac{R_L}{2}\frac{\partial a_i}{\partial \epsilon_L}\right) \tag{10}$$

In (10) above, we can safely assume for a steady equilibrium two-phase flow that the phasic properties remain fixed without interchange between phases. Consequently, we can claim that

$$(p_G - p_i) = -L_G\left(1 - \frac{R_G}{2}\frac{\partial a_i}{\partial \epsilon_G}\right) \tag{11}$$

$$(p_L - p_i) = L_L\left(1 + \frac{R_L}{2}\frac{\partial a_i}{\partial \epsilon_L}\right) \tag{12}$$

The above equations have the following consequences to be explained. Firstly, the surface tension thickness can be reversely obtained by

$$\delta = \frac{4\sigma}{(L_G + L_L)} \tag{13}$$

Equation (13) is, as a matter of fact, very close to an existing relation in the physical chemistry, namely,

$$l \approx \sigma\chi_t/2c \tag{14}$$

which is derived from the van der Waals/Cahn-Hilliard equation (Clive, 1980). Here c is a constant, χ_t is isothermal compressibility, and l is a measure of the interfacial thickness. It is, however, applicable when the liquid density is substantially larger than the gas density. Upon inserting physical data, (13) correctly verifies the physical observation that most liquids have surface thickness δ of an angstrom unit. Secondly, we find that the two-phase flow regimes can be obtained by different combination of the two bulk moduli, L_G and L_L. It is in contrast to other existing two-phase models. Thirdly, the experimental pressure-wave propagation can be correctly simulated by the present surface tension model. From (10)–(12), the relation between the phasic pressure jumps and the bulk moduli are obtained as follows

$$\frac{(p_G - p_i)}{(p_G - p_L)} = \frac{L_G}{L_G + L_L} \tag{15}$$

$$\frac{(p_i - p_L)}{(p_G - p_L)} = \frac{L_L}{L_G + L_L} \tag{16}$$

3. Characteristics of the hyperbolic equation system

Using the identity $\partial p_G/\partial x = \partial p_L/\partial x$ derived from (3) for the constants σ and δ, and the isentropic pressure-density relation $\partial p_k = \partial p_k/C_k^2$ where C_k is the sonic speed, we can rewrite the conservation equations as

$$\text{mass}: \quad \rho_k\frac{\partial\epsilon_k}{\partial t} + \frac{\epsilon_k}{C_k^2}\frac{\partial p_G}{\partial x} + \rho_k v_k\frac{\partial\epsilon_k}{C_k^2}\frac{\partial p_G}{\partial x} + \rho_k\epsilon_k\frac{\partial v_k}{\partial x} = \phi_{c,k} \tag{17}$$

$$\text{momentum}: \quad \epsilon_k\rho_k\frac{\partial v_k}{\partial t} + \epsilon_k\frac{\partial p_G}{\partial x} + \epsilon_k\rho_k v_k\frac{\partial v_k}{\partial x} + L_k\frac{\partial\epsilon_k}{\partial x} = (-1)^n L_k\frac{R_k}{2}\frac{\partial a_i}{\partial x} + \phi'_{m,k} \tag{18}$$

where $\phi_{m,k}$ is changed to a new term $\phi'_{m,k}$ to take the contribution from the mass source term $\phi_{c,k}$ into account. Also n is the exponent to distinguish the phasic states, with 1 for the gas and

2 for the liquid phase. The coupled quasi-linear partial differential equation system takes a compact matrix form

$$A\frac{\partial H}{\partial t}+B\frac{\partial H}{\partial x}=E \tag{19}$$

Here H is a state vector having four primitive variables, ϵ_G, p_G, u_G, and u_L; A and B are the coefficient matrices, and E is a source vector to be given by the empirical correlations. The eigenvalues λ of the coefficient matrix $G = A^{-1}$. B are determined from the characteristic equation, $\det(G-\lambda I) = 0$. A fourth-order polynomial equation is obtained as

$$P_4(\lambda)=(\lambda-\nu_G)^2(\lambda-\nu_L)^2-K_1(\lambda-\nu_G)^2-K_2(\lambda-\nu_L)^2+K_3 \tag{20}$$

where

$$K_1=\frac{L_L\epsilon_G C_L^2+C_G^2C_L^2\epsilon_L\rho_G}{\epsilon_G\rho_L C_L^2+\epsilon_L\rho_G C_G^2} \tag{21}$$

$$K_2=\frac{L_G\epsilon_L C_G^2+C_L^2C_G^2\epsilon_G\rho_L}{\epsilon_G\rho_L C_L^2+\epsilon_L\rho_G C_G^2} \tag{22}$$

$$K_3=\frac{C_G^2C_L^2(\epsilon_G L_L+\epsilon_L L_G)}{\epsilon_G\rho_L C_L^2+\epsilon_L\rho_G C_G^2} \tag{23}$$

The above characteristic equation has three sets of four distinct real eigenvalues that depend on the multipliers L_G and L_L. It is remarkable to note that these three distinct eigenvalue sets represent the three known two-phase flow regimes, namely the dispersed, the slug, and the separated flows. The eigenvalue sets are listed in Table 1.

Other than the above real eigenvalue sets, no other meaningful characteristic roots could be found due to the complexity of the equations. In the above, the multipliers, L_G and L_L, are obtained from the simplified physical models as follows.

Table 1
The distinct real eigenvalue sets dependent on L_k

Slug flow regime	$\lambda_{1,2}=\nu_G\pm C_L$ $\lambda_{3,4}=\nu_G\pm C_G$
Dispersed flow regime	$\lambda_{1,2}=\nu_L\pm C_L\sqrt{\dfrac{\rho_G C_G^2}{\epsilon_L\rho_G C_G^2+\epsilon_G\rho_L C_L^2}}$ $\lambda_{1,2}=\nu_G\pm C_G$
Separated flow regime	$\lambda_{1,2}=\nu_L\pm C_L\sqrt{\dfrac{\epsilon_L\rho_G C_G^2}{\epsilon_L\rho_G C_G^2+\epsilon_G\rho_L C_L^2}}$ $\lambda_{3,4}=\nu_G\pm C_G$

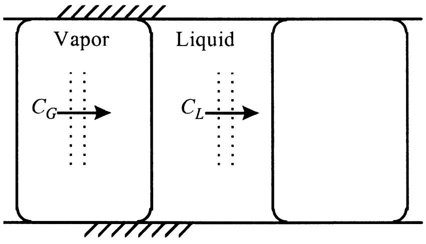

Fig. 2. Simplified physical model for the slug flow regime.

3.1. Slug flow

Since there is no elastic interaction between the two fluids and the sonic wave traveling in one fluid is not disturbed by the other fluid in the slug flow regime shown in Fig. 2, the time taken by the sonic wave to travel in the slug-flow column is equal to sum of the propagation time in each phase. Then the bulk modulus in each phase is identical to that of the single phase, namely,

$$L_G = \rho_G C_G^2 \tag{24}$$

$$L_L = \rho_L C_L^2 \tag{25}$$

3.2. Homogeneous flow

Mixture bulk modulus of the two fluids becomes

$$L_m = -V\frac{\mathrm{d}p}{\mathrm{d}V} = -V\frac{\mathrm{d}p}{\mathrm{d}V_L + \mathrm{d}V_G} = V\frac{\mathrm{d}p}{\dfrac{V_L\mathrm{d}p}{L_{L,s}} + \dfrac{V_G\mathrm{d}p}{L_{G,s}}} \tag{26}$$

where $V = V_G + V_L$ is the total volume of the mixture, and $L_{G,s}$ and $L_{L,s}$ are the bulk moduli of the single phases. For two phases of liquid and gas, it obviously holds that $L_{G,s} \ll L_{L,s}$. Then, (26) leads to

$$L_m = \frac{L_{G,s}}{\epsilon_G} \tag{27}$$

Equation (27) shows that the mixture bulk modulus is rather close to that of the gas than the liquid. Since the two fluids must have the same average bulk modulus for the homogeneous two fluids, it holds that $L_m = (L_L + L_G) \approx L_{G,s}/\epsilon_G$. Therefore, we can now set the bulk moduli as

$$L_G = \rho_G C_G^2 \tag{28}$$

$$L_L = \rho_G C_G^2 \frac{\epsilon_L}{\epsilon_G} \tag{29}$$

Assuming $\epsilon_G = \epsilon_L = 0.5$, we let $L_L = \rho_G C_G^2$. It will be observed later that this assumption of particular void fraction for L_L will not hamper the good comparison of the results with the experiment.

To be able to maintain perfect mixing, the characteristic length δ in (13) can be considered as a minimum distance separating the two fluids which have different bulk pressures due to the surface tension, that is,

$$\delta = \frac{2\sigma}{\rho_G C_G^2} \tag{30}$$

It is very exciting to note that this equation appears very close to the existing equation, $R_0 = 2\sigma T/\rho_2 h\theta_0$ (Van Stralen 1966), for the minimum radius of bubble nuclei in homogeneous nucleation process (see Blander and Katz, 1975). Here T, h and θ_0 are respectively the saturation temperature, latent heat of vaporization, and initial superheating temperature. Substituting the physical data, we find that both δ in (30) and R_0 have the same 10^{-6} m order of magnitude for many liquids. It is noted that the initial bubble nucleation in a liquid can therefore be expressed by a pure mechanical process.

3.3. Separated flow

In the case of the separated flow, it has been known that the pressure wave in gas is not transmitted into the liquid but most of the wave is reflected. Otherwise, it could be changed into capillary waves on the liquid surface. Unfortunately, the propagation mechanism of parallel pressure wave on the interface has not been well studied (Fig. 3). We set here the values of L_k approximately as follows:

$$L_G = \rho_G C_G^2 \tag{31}$$

$$L_L = 0 \tag{32}$$

On the other hand, Nguyen derived the sonic speed from the equations of continuity and momentum, considering a stationary wave front in a moving single phase medium as in Fig. 4.

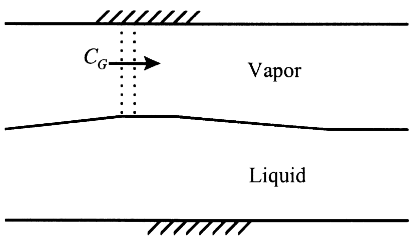

Fig. 3. Simplified physical model for the separated flow regime.

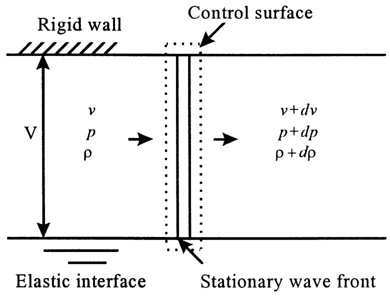

Fig. 4. Propagation model of an infinitesimal pressure pulse.

Combining of the continuity and momentum equations yields

$$v^2 = \frac{1}{\dfrac{\rho \mathrm{d}V}{V\mathrm{d}p} + \dfrac{\mathrm{d}\rho}{\mathrm{d}p}} = C^2 \tag{33}$$

Equation (33) depicts the effective sonic speed of the individual phase confined by an elastic boundary. The effective sonic speed depends upon the cross-sectional variation, $\mathrm{d}V/V$, or the

Table 2
Comparison of the effective sonic speeds in each phase

	Present model	Nguyen model
Slug flow regime (liquid/gas)	C_L	C_L
	C_G	C_G
Dispersed flow regime		
	$C_L\sqrt{\dfrac{\rho_G C_G^2}{\epsilon_L \rho_G C_G^2 + \epsilon_G \rho_L C_L^2}}$	$C_L\sqrt{\dfrac{\rho_G C_G^2}{\epsilon_L \rho_G C_G^2 + \epsilon_G \rho_L C_L^2}}$
	C_G	$C_G\sqrt{\dfrac{\rho_L C_L^2}{\epsilon_L \rho_G C_G^2 + \epsilon_G \rho_L C_L^2}}$
Separated flow regime		
	$C_L\sqrt{\dfrac{\epsilon_L \rho_G C_G^2}{\epsilon_L \rho_G C_G^2 + \epsilon_G \rho_L C_L^2}}$	$C_L\sqrt{\dfrac{\epsilon_L \rho_G C_G^2}{\epsilon_L \rho_G C_G^2 + \epsilon_G \rho_L C_L^2}}$
	C_G	$C_G\sqrt{\dfrac{\epsilon_G \rho_L C_L^2}{\epsilon_L \rho_G C_G^2 + \epsilon_G \rho_L C_L^2}}$

Table 3
Comparison of the effective sonic speeds in the limiting cases

	Present model				Nguyen model			
	$\epsilon\to 0$		$\epsilon\to 1$		$\epsilon\to 0$		$\epsilon\to 1$	
	gas	Liquid	gas	Liquid	gas	Liquid	gas	Liquid
Slug flow	C_G	C_L	C_G	C_L	C_G	C_L	C_G	C_L
Homogeneous flow	C_G	C_L	C_G	$C_G\sqrt{\frac{\rho_G C_G^2}{\rho_L C_L^2}}$	$* \, C_G\sqrt{\frac{\rho_L C_L^2}{\rho_G C_G^2}}$	C_L	C_G	$C_G\sqrt{\frac{\rho_G C_G^2}{\rho_L C_L^2}}$
Separated flow	C_G	C_L	C_G	0	0	C_L	C_G	0

Physically the effective sonic speed cannot be larger than that of the single phase. However, as marked with *, Nguyen's model gives sonic speed for the gas in homogeneous flow much greater than C_G or even C_L.

void-fraction variation which is replaced by a reasonable physical model for each flow regime. These Nguyen's values are compared with the present results in Table 2.

The basic difference between the two physical models is that Nguyen does not consider the interfacial discontinuity of the momentum caused by the surface tension. If the surface tension can be ignored (when bubble size is large enough to separate), Nguyen's result could be more accurate than the present one. However, Nguyen's result shows such nonphysical phenomenon that the sonic speed of gas is greater than that of the single phase at the limiting state ($\epsilon\to 0$) in

Table 4
Comparison of total speed of sound

Flow regimes	Models	
	Present results	Theoretical results by Nguyen et al.
Slug flow	$C_i = \frac{C_G C_L}{\epsilon_L C_G + \epsilon_G C_L}$	$C_i = \frac{C_G C_L}{\epsilon_L C_G + \epsilon_G C_L}$
Dispersed flow	$C_i = \frac{C_G C_L\sqrt{\frac{\rho_G C_G^2}{\epsilon_L\rho_G C_G^2+\epsilon_G\rho_L C_L^2}}}{\epsilon_L C_G + \epsilon_G C_L\sqrt{\frac{\epsilon_L\rho_G C_G^2}{\epsilon_L\rho_G C_G^2+\epsilon_G\rho_L C_L^2}}}$	$C_i = \frac{C_G C_L\sqrt{\frac{\rho_G C_G^2}{\epsilon_L\rho_G C_G^2+\epsilon_G\rho_L C_L^2}}}{\epsilon_L\sqrt{\epsilon_G\rho_L} + \epsilon_G\sqrt{\epsilon_L\rho_G}}$
Separated flow	$C_i = \frac{C_G C_L\sqrt{\frac{\epsilon_L\rho_G C_G^2}{\epsilon_L\rho_G C_G^2+\epsilon_G\rho_L C_L^2}}}{\epsilon_L C_G + \epsilon_G C_L\sqrt{\frac{\epsilon_L\rho_G C_G^2}{\epsilon_L\rho_G C_G^2+\epsilon_G\rho_L C_L^2}}}$	$C_i = \frac{C_G C_L\sqrt{\frac{\epsilon_G\epsilon_L\rho_G C_G^2}{\epsilon_L\rho_G C_G^2+\epsilon_G\rho_L C_L^2}}}{\epsilon_L\sqrt{\epsilon_G\rho_L} + \epsilon_G\sqrt{\epsilon_L\rho_G}}$

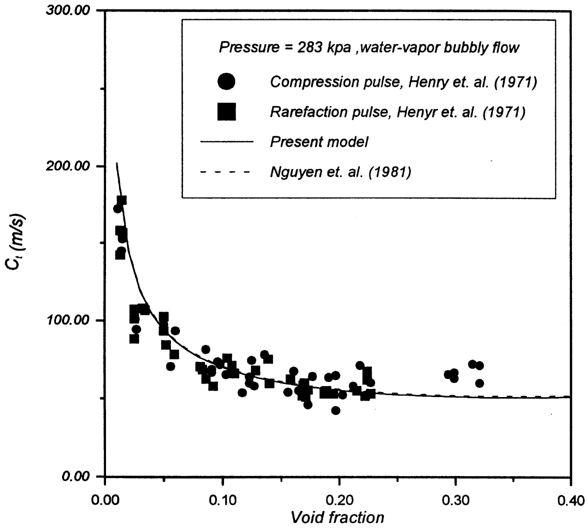

Fig. 5. Total speed of sound: water-vapor dispersed flow.

the homogeneous flow regime (Table 3). In contrast, the present model suggests adequate values in all of the flow regimes.

To test the accuracy of the present theory, the eigenvalues are compared with both the experimental speeds of sound measured by Henry et al. (1971) and the theoretical results by Nguyen et al. (1981). For this purpose, we first define a total speed of sound, weighted by the

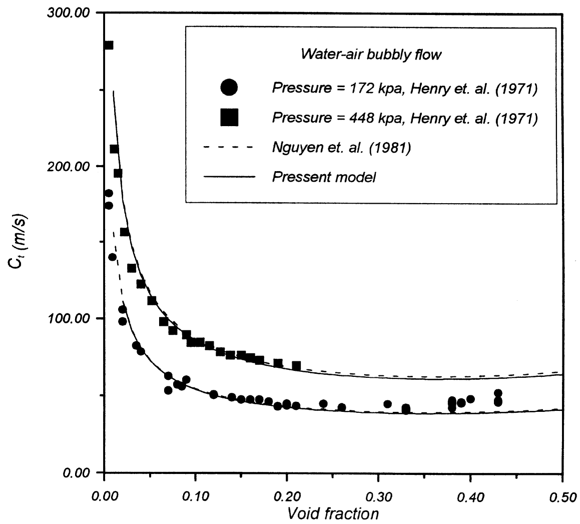

Fig. 6. Total speed of sound: water-air dispersed flow.

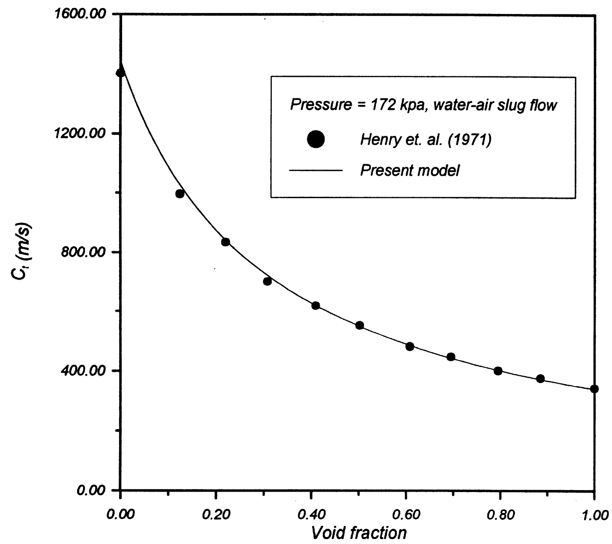

Fig. 7. Total speed of sound: water-air slug flow.

void fraction of the individual phase:

$$C_t = \frac{\lambda_1 \lambda_3}{\epsilon_L \lambda_3 + \epsilon_G \lambda_1} \tag{34}$$

Table 4 compares the present total speed of sound with that of Nguyen et al. The present result shows good agreement with both Nguyen et al.'s and experimental values for both the

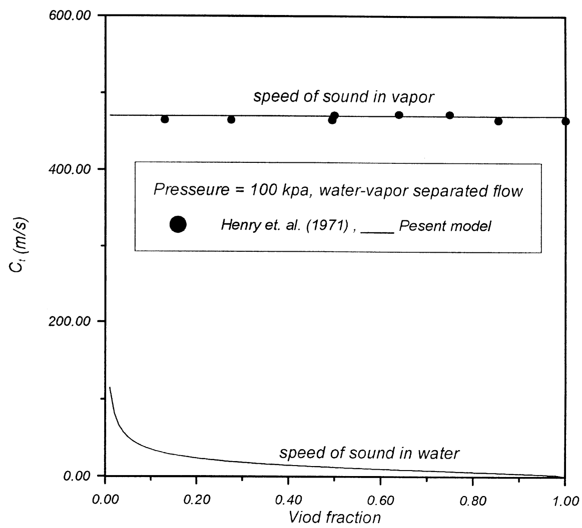

Fig. 8. Total speed of sound: water-vapor separated flow.

water-vapor flow in Fig. 5 and water-air dispersed flows in Fig. 6. Figs. 7 and 8 show the total speed of sound agreeing well with the experimental values for other flow regimes like water-air slug flow and water-vapor separated flow.

4. Conclusions

We have theoretically predicted the phasic speeds of sound in the two-phase mixture by means of the eigenvalues of the two fluids equation system. The pressure discontinuity at the interface which is properly treated using the surface physics resulted in excellent agreement of the present results with the experiment. Although application of the present theory is made to a two-phase acoustic problem in this paper, transient two-phase flow regimes can be treated in the future.

References

Aubin, J.P., Ivar, Ekeland 1984. Applied Nonlinear Analysis, Chap. 4. John Wiley, New York.

Blander, M., Katz, J.L., 1975. Bubble nucleation in liquid. AIChE J 21, 833–848.

Clive, A. 1980. Statistical Mechanics of the Liquid Surface, Chap. 1. Wiley, New York.

Delhaye, J.M., Giot, M., Riethmuller, M.L. 1981. Thermohydraulics of Two-Phase Systems for Industrial Design and Nuclear Engineering, Chap. 7. McGraw-Hill, New York.

Egelstaff, P.A., Widom, B., 1970. Liquid surface tension near the triple point. J. Chem. Phys. 53, 2667–2669.

Henry, R.E., Grolenes, M.A., Fauske, H.K. 1971. Pressure-pulse propagation in two-phase one- and two-component mixtures. ANL-7792.

Holm, D.D., Kupershmidt, B.A., 1986. A multipressure regularization for multiphase flow. Int. J. Multiphase Flow 12, 681–897.

Ishii, M. 1975. Thermo-Fluid Dynamic Theory of Two-Phase Flow. Eyrulles, Paris.

Nguyen, K.L., Winter, E.R.F., Greiner, M., 1981. Sonic velocity in two-phase systems. Int. J. Multiphase Flow 7, 311–320.

Papalambros, Y.P., Douglass, J.W. 1988. Principles of Optimal Design. Cambridge University Press.

Present, R.D.J., 1974. On the product of surface tension and compressibility of the liquids. J. Chem. Phys. 61, 4267–4269.

Ramshaw, J.D., Trapp, J.A., 1978. Characteristics, stability, and short-wavelength phenomena in two-phase flow equation systems. Nuclear Sci. and Eng. 66, 93–102.

Ramsom, V.H., Hicks, D.L., 1984. Hyperbolic two-pressure models for two-phase flow. J. Comput. Phys. 53, 124–151.

Stewart, H.B., 1979. Stability of two-phase flow calculation using two-fluid models. J. Comput. Phys. 33, 259–270.

Van Stralen, S.J.D., 1966. The mechanism of nucleate boiling in pure liquids and in binary mixtures. Pt. I and Pt. II. Int. J. Heat and Mass Transfer 9, 995–1046 .